


Adaptive Time-Varying Parameter Estimation via Weak Measurement

Qi Song[✉], Hongjing Li,^{*} Jingzheng Huang, Tailong Xiao, Xiaorui Tan, Binke Xia, and Guihua Zeng[†]
State Key Laboratory of Advanced Optical Communication Systems and Networks, School of Electronic Information and Electrical Engineering, Institute of Quantum Sensing and Information Processing, Shanghai Jiao Tong University, Shanghai 200240, People's Republic of China

 (Received 8 June 2022; revised 9 August 2022; accepted 6 September 2022; published 13 October 2022)

Extending quantum sensing to time-varying parameter estimation is a potential and challenging task in practical application. To achieve this goal, we propose an adaptive method to estimate an unknown time-varying parameter through light-intensity split detection and the insertion of reference phases in the weak measurement. Theoretical analysis and numerical simulation are applied to illustrate the feasibility and practical applications of our method. The results demonstrate that the method has adjustable sensitivity and linear dynamic range, and is robust to nonideal measurement conditions. Moreover, we analyze the precision of our method and show that its precision limit can surpass the standard quantum limit and approach the Heisenberg scaling when using a squeezed light of optimal Gaussian state.

DOI: [10.1103/PhysRevApplied.18.044031](https://doi.org/10.1103/PhysRevApplied.18.044031)

I. INTRODUCTION

Quantum sensing focuses on performing a higher sensitivity and precision measurement of a physical quantity with the application of quantum system and resources. Two of the most useful features of quantum sensing are strong response to signals and minimal interference with unwanted noise [1,2]. Usually, the quantum sensing process can be divided into four steps: the preparation of the probe state, the parameterization of the signals of interest, the readout of the final state, and classical statistical processing [2,3]. For many applications, such as quantum navigation, quantum lidar, atomic clocks, etc. [4], the signals of interest are unknown, stochastic, and time varying. Much research in recent years indicates that the estimation of a time-varying parameter has more potential and is more challenging than the well-established static and deterministic parameter estimation [2–6]. It is generally accepted that the prior information and data processing of the time-varying parameters need to be taken into account in the estimation [3,5–8]. Tsang *et al.* [7] took the prior information of parameters as a part of Fisher information matrix and gave an alternative quantum Cramér-Rao bound (QCRB). Berry *et al.* [8] also considered the prior information and demonstrated the standard quantum limit scaling and the Heisenberg scaling of a stationary Gaussian stochastic phase with a power-law spectrum. Kura *et al.* [6] analyzed the case of data postprocessing of function

smoothing, and gave an alternative standard quantum limit (SQL) and Heisenberg limit (HL) under different degrees of the function smoothness.

In order to measure a time-varying parameter, two conditions should be satisfied. The first condition is the changing speed of the parameter can be tracked by detectors, which is bound by the Nyquist sampling theorem [6,9,10]. The second condition is the amplitude of the parameter at any time can be detected by the measurement scheme. Previous estimation methods for quantum time-varying parameters can be divided into two categories. One focuses on the evolution process and estimates the parameters in time-dependent Hamiltonians [11,12], where the accurate compensation of the optimal Hamiltonian control and the real-time acquisition of Fisher information are difficult to accomplish in practice. The other one focuses on independent measurement and synthesizes the results to realize time-varying parameter estimation. Among them, much research focus on the precision improvement of the adaptive time-varying phase-estimation method based on heterodyne detection through using a quantum light source and improving the optical structure continuously [5,13–16]. Berry *et al.* [14] analyzed the feasibility of the scheme with coherent light and squeezed light, and demonstrated the theoretical precision limits. Dinani *et al.* [15] showed that the Heisenberg scaling can be achieved via squeezed state. Zheng *et al.* [5] confirmed that the use of nonlinear interferometer can achieve stochastic Heisenberg scaling, and has a better SNR than the Mach-Zehnder interferometer. However, the measurement precision and sensitivity of this method depend on the adaptive phase, which may limit some applications of the method.

^{*}lhjnet2012@sjtu.edu.cn

[†]ghzeng@sjtu.edu.cn

In this paper, we propose an adaptive method via weak measurement to estimate an unknown time-varying phase. Compared with original weak measurement, the method replaces spectral detection with light-intensity detection, which enables the signal with a higher frequency. With the insertion of reference phases, the method can measure parameters with an adjustable sensitivity and dynamic range, which enables a signal with a larger amplitude. The method is also robust against relative intensity noise (RIN) and nonideal detection conditions. When applying a squeezed light of optimal Gaussian state as the light source, the precision limit of the method can surpass the SQL and approach the Heisenberg scaling.

The paper is organized as follows. After the introduction in Sec. I, Sec. II proposes the method and verifies its feasibility and advantages of adjustable sensitivity and dynamic range through numerical simulation. The precision and robustness of the method are analyzed in Sec. III and Sec. IV, respectively. Finally, we conclude by summarizing our contributions in Sec. V.

II. THEORETICAL SCHEME SETUP

In this section, we develop a general theory for the estimation of an unknown time-varying parameter based on weak measurement technique [17–21]. We assume $x(t)$ is the time-varying parameter to be estimated, and sample it with equal interval, which determines the frequency of the parameters can be detected [10]. $x(t)$ can be denoted as $\{x(t_1), x(t_2), \dots, x(t_j), \dots\}$, and estimated by a set of observations $\{\gamma(t_1), \gamma(t_2), \dots, \gamma(t_j), \dots\}$, where t_j means the sampling instant. As the minimum detection time for a single detection of light-intensity detection is much lower than spectrum detection, light-intensity detection enables time-varying parameters with a higher frequency. Thus, we choose light intensity as the observable.

The process of our method is depicted in Fig. 1, the light beam is modulated as $|i\rangle = 1/\sqrt{2}(|H\rangle + |V\rangle)$ in the preselection. In the weak interaction process, a signal is encoded into a time-varying phase parameter, which introduces $\varphi(t)$ between $|H\rangle$ and $|V\rangle$. The polarization state of the light beam evolves into

$$|\Psi_i(t)\rangle = e^{-i\varphi(t)\hat{A}} |i\rangle, \quad (1)$$

where the Stokes polarization operator $\hat{A} = |H\rangle\langle H| - |V\rangle\langle V|$ acts on the system. After that, it is split into two paths by a beam splitter (BS), the first and second path are distinguished by 1 and 2 in subscripts.

In order to make the scheme have adjustable sensitivity and liner dynamic range, a reference phase is inserted into each path [22], and the time evolution caused by the reference phases can be expressed as

$$\hat{U}_{r,1,2}(t) = e^{-i\varphi_{r,1,2}(t)\hat{A}}, \quad (2)$$

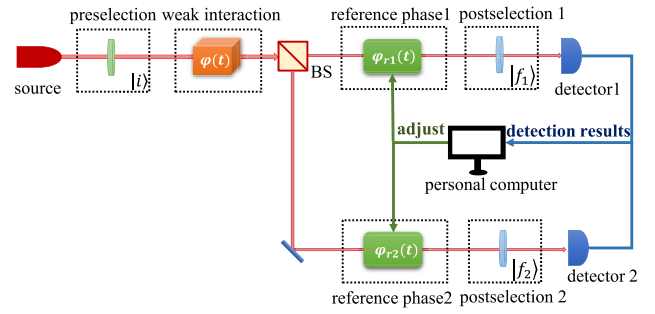


FIG. 1. Schematic diagram of adaptive time-varying phase-estimation method via weak measurement. An unknown time-varying phase $\varphi(t)$ is introduced in the weak interaction. The light is split into two paths through a beam splitter and projected to two postselection states for detection. The value of reference phases is adjusted in real time according to the relationship between recent measurement value and the presupposed threshold of specific requirements.

and the light beam evolves into

$$\begin{aligned} |\Psi_{1,2}(t)\rangle &= \hat{U}_{r,1,2}(t) |\Psi_i(t)\rangle \\ &= \hat{U}_{r,1,2}(t) e^{-i\varphi(t)\hat{A}} |i\rangle. \end{aligned} \quad (3)$$

In particular, the adjustment of reference phase is an adaptive process, where the value of reference phases is adjusted in real time according to the relationship between recent measurement value and the presupposed threshold of specific requirements.

In the postselection process, the evolved state $|\Psi_{1,2}(t)\rangle$ is projected to final state $|f_{1,2}\rangle = 1/\sqrt{2}(ie^{i\varepsilon_{1,2}}|H\rangle - ie^{-i\varepsilon_{1,2}}|V\rangle)$, which is nearly orthogonal to the preselection and $\varepsilon_{1,2}$ is the postselection angle of each path. For facilitating calculation, the reference phase and postselection angle of each path should be opposite [23,24]

$$\begin{aligned} \varphi_{r,1,2}(t) &= \pm\varphi_r(t), \\ \varepsilon_{1,2} &= \pm\varepsilon. \end{aligned} \quad (4)$$

After postselection, the light intensity of each path is

$$\begin{aligned} I_{1,2}(t) &= \frac{I_0}{2} |\langle f_{1,2} | \Psi_{1,2}(t) \rangle|^2 \\ &= \frac{I_0}{2} \{ \sin^2[\varepsilon + \varphi_r(t)] \cos^2[\varphi(t)] \\ &\quad + \cos^2[\varepsilon + \varphi_r(t)] \sin^2[\varphi(t)] \\ &\quad \pm \frac{1}{2} \sin[2\varphi(t)] \sin[2\varepsilon + 2\varphi_r(t)] \}, \end{aligned} \quad (5)$$

where I_0 is the initial light intensity. In order to facilitate data postprocessing, the intensity contrast ratio

$$\xi = \frac{I_1 - I_2}{(I_1 + I_2)/2} \quad (6)$$

is adopted as the index of observation, and the corresponding intensity contrast ratio can be expressed as

$$\xi(t) = \frac{\sin[2\varphi(t)] \sin[2\varepsilon + 2\varphi_r(t)]}{\sin^2[\varepsilon + \varphi_r(t)] \cos^2[\varphi(t)] + \cos^2[\varepsilon + \varphi_r(t)] \sin^2[\varphi(t)]}. \quad (7)$$

Here, $\varphi_r(t) = \tilde{\varphi}_r(t) + m\pi$, $\varphi(t) = \tilde{\varphi}(t) + n\pi$, where m and n mean integers, $\tilde{\varphi}_r(t)$ and $\tilde{\varphi}(t)$ range from $-\pi/2$ to $\pi/2$.

In particular, under the condition of

$$|\tilde{\varphi}(t)| \ll \left| \frac{1}{\text{Im}A_{w1,2}(t)} \right|, \quad (8)$$

where

$$\begin{aligned} A_{w1,2}(t) &= \frac{\langle f_{1,2} | \hat{U}_{r1,2}(t) \hat{A} | i \rangle}{\langle f_{1,2} | \hat{U}_{r1,2}(t) | i \rangle} \\ &= \pm i \cot[\varepsilon + \varphi_r(t)] \end{aligned} \quad (9)$$

is the so-called weak value of each path, the light intensity of each path can be approximated to

$$I_{1,2}(t) \approx \frac{I_0}{2} \sin^2[\varepsilon + \varphi_r(t)] [1 + 2\tilde{\varphi}(t) \text{Im}A_{w1,2}(t)], \quad (10)$$

and $\xi(t)$ can be expressed as

$$\xi(t) \approx 4\tilde{\varphi}(t) \cot[\varepsilon + \varphi_r(t)]. \quad (11)$$

As a result, the system operates in a linear dynamic range with the detection sensitivity

$$\frac{\delta\xi}{\delta\tilde{\varphi}} = 4 \cot[\varepsilon + \varphi_r(t)], \quad (12)$$

indicating that the measurement can also achieve a high sensitivity even if $\varphi(t)$ exceeds the range of $\tilde{\varphi}(t)$, as depicted in Fig. 2(a).

Based on the above equations, the measurement sensitivity in the linear dynamic range is dependent on the value of $\varphi_r(t) + \varepsilon$. As the adjustment of reference phases is easier than the postselection angle in practice, we can adjust the value of reference phase according to the measuring results to control the measurement in a wider or a much more sensitive dynamic range, as depicted in Fig. 2(b).

In order to demonstrate the advantages of the insertion of reference phases, a numerical simulation is designed. Here, $\varphi(t)$ is set as $\varphi(t) = 0.002 \cos(2\pi ft - \pi/3)$ (rad), where $f = 1$ kHz, and part of it exceeds the original linear range when postselection angle is set as $\varepsilon = 0.001$. As shown in Fig. 3, the simulation results show that the measurement sensitivity and linear dynamic range can be controlled with the reference phases, which enables the method to be more adaptable to unknown time-varying parameters.

Indeed, how to introduce and control reference phases is the main experimental challenge of the method. On one hand, the adjustment speed is related to the maximum signal frequency that the method can detect. On the other hand, reference phases can also affect the actual precision of the method. It is difficult to ensure the reference phases of the two paths introduced during adjustment are opposite. However, these challenges can be overcome with the development of adjustable and controlled instruments.

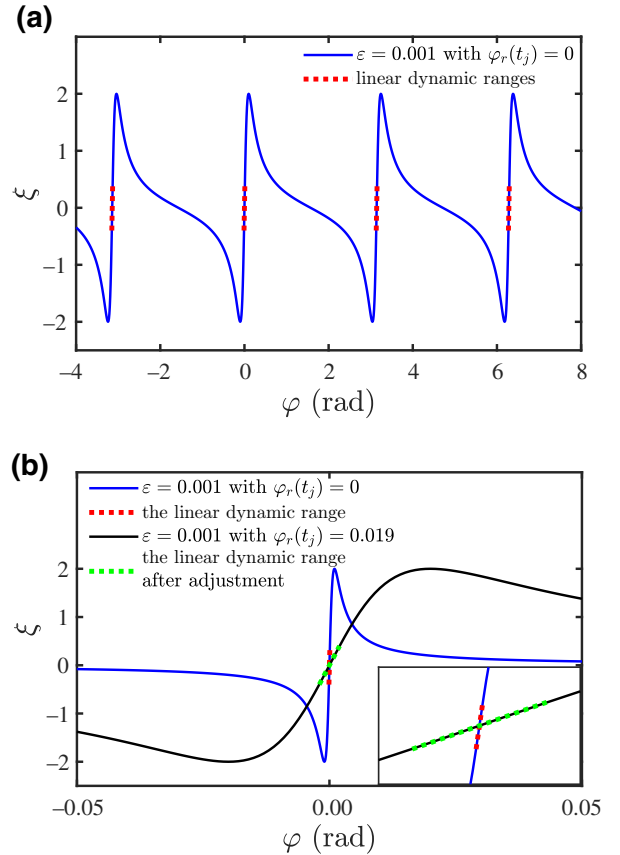


FIG. 2. The blue line depicted in (a) shows the relationship between ξ and φ when setting $\varepsilon = 0.001$ with $\varphi_r(t_j) = 0$, and the red dotted lines show the linear dynamic range. The adjustment effect of reference phases is depicted in (b), where the black line shows the relationship while the green dotted line marks the linear dynamic range after adjustment. The enlargement of the linear dynamic range is depicted in the right bottom of (b).

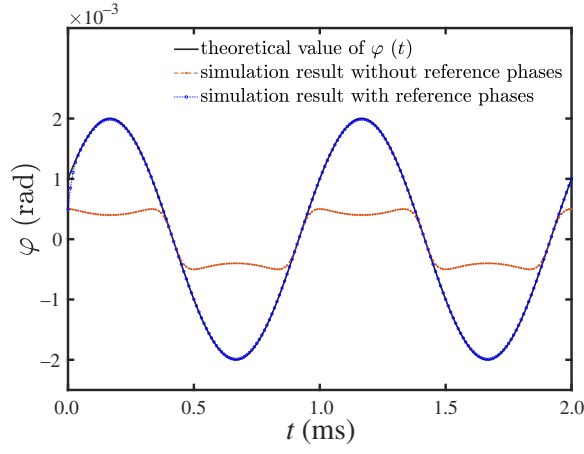


FIG. 3. Simulation results of the time-varying phase with and without reference phases. The black line represents the theoretical value of $\varphi(t)$, while the blue dotted line with circles and the red dashed line with points represent the estimated values with and without reference phases, respectively.

III. PRECISION LIMIT ANALYSIS

In this section, a theoretical analysis is carried out to derive the precision limit of the method. In the weak interaction process, the weak measurement will change the particle-number distribution when we choose the light intensity as the observable [21]. The interaction Hamiltonian can be expressed as [20,21]

$$H(t_j) = \varphi(t_j)\delta(t - t_j)\hat{A}\hat{n}, \quad (13)$$

where the particle number operator \hat{n} is the observable of the pointer, and $\delta(t - t_j)$ indicates the interaction happens at the time of t_j . As the Hamiltonian at arbitrary two time t_j and t_k satisfies $[H(t_j), H(t_k)] = 0$, the time-varying parameter estimation can be considered as a multiparameter estimation in the time dimension. Thus, the Hamiltonian in the time dimension can be given as

$$H_t = \sum_{t_j} \varphi(t_j)\delta(t - t_j)\hat{A}_{t_j}\hat{n}_{t_j}, \quad (14)$$

and the time evolution can correspondingly be written as

$$\hat{U}_t = e^{-i\sum_{t_j} \varphi(t_j)\hat{A}_{t_j}\hat{n}_{t_j}}. \quad (15)$$

We employ quantum Fisher information matrix (QFIM), whose inverse is the QCRB, as the figure of merit to evaluate the statistical error of the time-varying parameter estimation [3,7,25].

When the weak measurement meets Eq. (8), the final state of each path can be approximated to [19]

$$\begin{aligned} |\phi_{f,1,2}\rangle &= \langle f_{1,2}|\hat{U}_{r,1,2}(t)\hat{U}_r|i\rangle|\phi_i\rangle \\ &\approx \langle f_{1,2}|\hat{U}_{r,1,2}(t)|i\rangle e^{-i\sum_{t_j} \varphi(t_j)A_{w,1,2}(t_j)\hat{n}_{t_j}}|\phi_i\rangle, \end{aligned} \quad (16)$$

where the normalized factor can be approximately given by $\langle f_{1,2}|\hat{U}_{r,1,2}(t)|i\rangle$ and it can be normalized as

$$|\phi_{n,1,2}\rangle = e^{-i\sum_{t_j} \varphi(t_j)A_{w,1,2}(t_j)\hat{n}_{t_j}}|\phi_i\rangle. \quad (17)$$

The QFIM of the pure $\varphi(t_j)$ -dependent state $|\phi_{n,1,2}\rangle$ [3] can be expressed as

$$\begin{aligned} Q_{1,2}(t_j, t_k) &= 4\text{Re}\langle \partial_{\varphi(t_j)}\phi_{n,1,2}|\partial_{\varphi(t_k)}\phi_{n,1,2}\rangle \\ &\quad - 4\text{Re}\langle \partial_{\varphi(t_j)}\phi_{n,1,2}|\phi_{n,1,2}\rangle\langle \phi_{n,1,2}|\partial_{\varphi(t_k)}\phi_{n,1,2}\rangle \\ &\approx 4A_{w,1,2}^*(t_j)A_{w,1,2}(t_k)\delta(t_j - t_k)(\langle \phi_i|\hat{n}^2|\phi_i\rangle \\ &\quad - \langle \phi_i|\hat{n}|\phi_i\rangle^2) \\ &= 4A_{w,1,2}^*(t_j)A_{w,1,2}(t_k)\delta(t_j - t_k)\langle \phi_i|\Delta\hat{n}|\phi_i\rangle^2, \end{aligned} \quad (18)$$

whose nondiagonal elements are 0.

Moreover, the total QFIM of $\varphi(t)$ can be given by [21,26]

$$F^Q(t_j, t_k) = p_{s1}(t_j, t_k)Q_1(t_j, t_k) + p_{s2}(t_j, t_k)Q_2(t_j, t_k). \quad (19)$$

Here, $p_{s1,2}(t_j, t_k)$ is the actual detection probability, whose diagonal elements represent the probability at the time of t_j

$$\begin{aligned} p_{s1,2}(t_j, t_j) &\approx \frac{1}{2}|\langle f_{1,2}|\hat{U}_{r,1,2}(t_j)|i\rangle|^2 \\ &= \frac{1}{2}\sin^2[\varepsilon + \varphi_r(t_j)]. \end{aligned} \quad (20)$$

Thus, the nondiagonal elements $F^Q(t_j, t_k)(j \neq k)$ are 0, and the diagonal elements of F^Q can be expressed as

$$F^Q(t_j, t_j) = 2\{1 + \cos[2\varepsilon + 2\varphi_r(t_j)]\}\langle \phi_i|\Delta\hat{n}|\phi_i\rangle^2, \quad (21)$$

which is the quantum Fisher information of $\varphi(t_j)$.

Based on Eq. (21), it can be found that the precision limit of each measurement is related to $\langle \phi_i|\Delta\hat{n}|\phi_i\rangle^2$. When we employ coherent state as the initial state $|\phi_i\rangle$ with a number of N photons per coherence time, the precision limit $\propto N^{-1/2}$, which can reach the SQL. In particular, if a squeezed light source of the optimal Gaussian state [27]

is employed in our method, its precision can be enhanced. The diagonal elements of F^Q can be written as

$$F^Q(t_j, t_j) = 4\{1 + \cos[2\varepsilon + 2\varphi_r(t_j)]\}(n_r^2 + n_r), \quad (22)$$

where $n_r = \sinh^2(r)$ is the mean photon number and r is the squeezing parameter [27,28], and it can be approximated to

$$F^Q(t_j, t_j) \approx 4\{1 + \cos[2\varepsilon + 2\varphi_r(t_j)]\}n_r^2 \quad (23)$$

for n_r is large enough. Accordingly, the precision limit $\propto n_r^{-1}$, which surpasses the SQL and approaches the Heisenberg scaling [29].

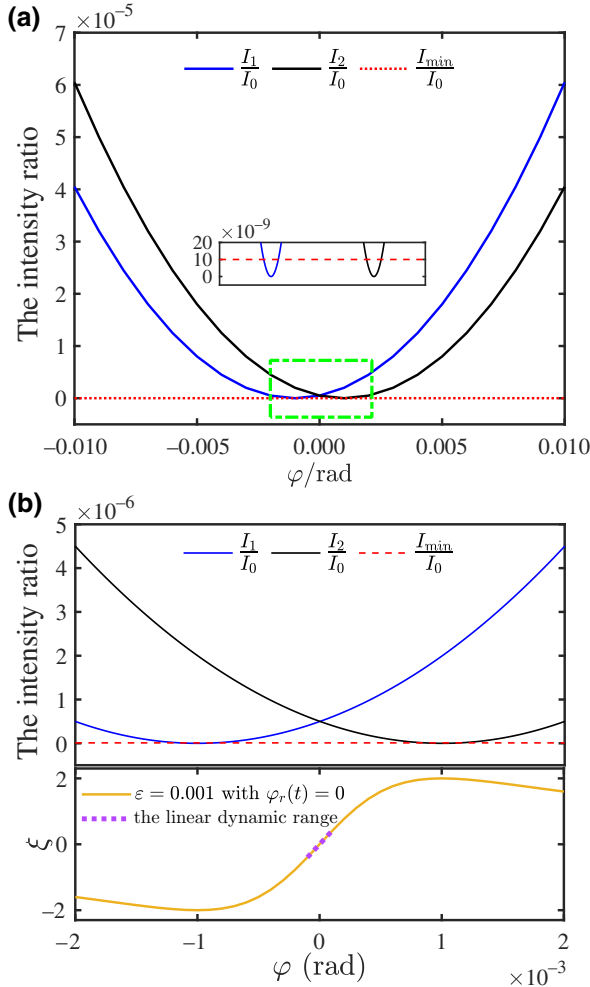


FIG. 4. Relationship between I_1/I_0 (blue line), I_2/I_0 (black line), and φ is depicted in (a), which is highlighted when I_1/I_0 and I_2/I_0 are lower than I_{\min}/I_0 (the red dotted line) at the top. The part surrounded by the green border is selected to generate (b) and the relationship between ξ and the corresponding φ to facilitate observation is depicted at the bottom of (b) (the yellow line), where the purple dashed line shows the liner dynamic range. Here, $\varepsilon = 0.001$.

IV. ROBUSTNESS ANALYSIS

In this section, the applicability of the method in practical conditions is analyzed rather than the ideal measurement situation analysis in previous sections. At first, we consider the RIN of the light source, which obeys Gaussian distribution and leads to the power fluctuation of the light source. The output light intensity can be expressed as

$$I_0(t) = \bar{I}_0 + \Delta I_0(t), \quad (24)$$

where \bar{I}_0 is the ideal output light intensity, and $\Delta I_0(t)$ is the RIN. As shown in Eq. (7), the real-time values of the time-varying parameters are obtained by calculating the intensity contrast of the two paths. As the power fluctuation of the light source does not affect the estimation of the time-varying parameter, the method can effectively eliminate the RIN.

Then we consider the nonideal detection conditions, where the minimum detectable light intensity I_{\min} and detection errors $\Delta I(t)$ exist. The final light intensity of each path can be expressed as

$$I_{1,2}(t) = \bar{I}_{1,2}(t)[1 + \Delta I(t)], \quad (25)$$

where $\bar{I}_{1,2}(t)$ is the ideal output light intensity expressed in Eq. (5), and $\Delta I(t)$ has an upper bound expressed as a percentage, which obeys Gaussian distribution. As shown in Fig. 4, the minimum detectable light intensity I_{\min} has almost no effect in the linear dynamic range, but the impact of detection errors $\Delta I(t)$ is large when the light intensity of

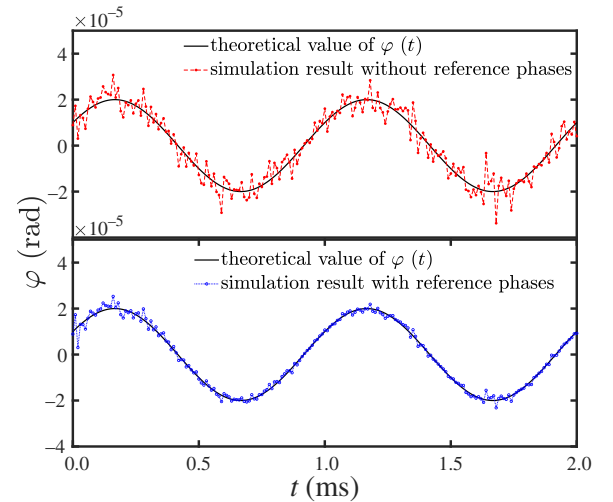


FIG. 5. Simulation results of the time-varying phase with and without reference phases under the condition of detection errors. The black line represents the theoretical value of $\varphi(t)$, the blue dotted line with circles and the red dashed line with points represent the estimated values with and without reference phases, respectively. Here, $\varepsilon = 0.001$.

TABLE I. Calculation results of similarity and errors for the time-varying phase estimation with detection errors.

	r	MAE (μrad)	RMSE (μrad)
Simulation result without reference phases	0.9855	1.8719	2.4434
Simulation result with reference phases	0.9962	0.7626	1.2439

two paths are close. Therefore, we focus on the robustness of our method against detection errors.

In order to testify the validity of our method under the condition of detection errors, a numerical simulation is carried out. $\varphi(t)$ is set as $\varphi(t) = 20 \cos(2\pi ft - \pi/3)$ (μrad), where $f = 1$ kHz, and we assume that the detection error has an upper bound of 2%. The simulation results are shown in Fig. 5, and we can observe that the simulation result with the insertion of reference phases is closer to $\varphi(t)$.

As listed in Table I, three figures of merit are introduced to evaluate the performance of our method precisely. The correlation coefficient, denoted as r , evaluates the similarity between the estimated value and the true value, while root-mean-square error (RMSE) and mean absolute error (MAE) evaluates the errors quantificationally. The calculation results show that our method maintains good performance even when detection errors exist, which implies its robustness to nonideal detection condition with the insertion of reference phases.

V. CONCLUSION

In summary, considering the requirement of amplitude and frequency on time-varying parameter detection, we propose an adaptive time-varying parameter-estimation method through light-split detection and the insertion of reference phases in the weak measurement. The method can detect the parameter with adjustable sensitivity and linear dynamic range in real time. The precision limit of our method is analyzed via QFIM, which can be enhanced by using nonclassical resources. For example, our method can surpass the SQL and approach the Heisenberg scaling by using a squeezed light source of the optimal Gaussian state. In addition, the robustness of the method against nonideal measurement conditions is also analyzed. The effect of RIN and the minimum detectable intensity of detectors can be effectively eliminated with the application of intensity contrast index, and detection errors can also be suppressed by inserting the reference phases. The analysis results indicate the practical application of our method in time-varying parameter estimation.

ACKNOWLEDGMENTS

This work is supported by the National Natural Science Foundation of China (Grants No. 61901258 and No. 62071298).

- [1] V. Giovannetti, S. Lloyd, and L. Maccone, Quantum Metrology, *Phys. Rev. Lett.* **96**, 010401 (2006).
- [2] C. L. Degen, F. Reinhard, and P. Cappellaro, Quantum sensing, *Rev. Mod. Phys.* **89**, 035002 (2017).
- [3] J. Liu, H. Yuan, X. Lu, and X. Wang, Quantum Fisher information matrix and multiparameter estimation, *J. Phys. A: Math. Theor.* **53**, 023001 (2019).
- [4] *OIDA Quantum Photonics Roadmap: Every Photon Counts*, OSA Industry Development Associates 20202020.
- [5] K. Zheng, M. Mi, B. Wang, L. Xu, L. Hu, S. Liu, Y. Lou, J. Jing, and L. Zhang, Quantum-enhanced stochastic phase estimation with the Su(1, 1) interferometer, *Photonics Res.* **8**, 1653 (2020).
- [6] N. Kura and M. Ueda, Standard Quantum Limit and Heisenberg Limit in Function Estimation, *Phys. Rev. Lett.* **124**, 010507 (2020).
- [7] M. Tsang, H. M. Wiseman, and C. M. Caves, Fundamental Quantum Limit to Waveform Estimation, *Phys. Rev. Lett.* **106**, 090401 (2011).
- [8] D. W. Berry, M. J. W. Hall, and H. M. Wiseman, Stochastic Heisenberg Limit: Optimal Estimation of a Fluctuating Phase, *Phys. Rev. Lett.* **111**, 113601 (2013).
- [9] H. Nyquist, Certain topics in telegraph transmission theory, *Trans. Am. Inst. Electr. Eng.* **47**, 617 (1928).
- [10] J. Zheng, Q. Ying, and W. Yang, *Signal and System* Vol. 1 (Higher Education Press, Beijing, 2011), 3rd ed.
- [11] S. Pang and A. N. Jordan, Optimal adaptive control for quantum metrology with time-dependent hamiltonians, *Nat. Commun.* **8**, 1 (2017).
- [12] T. Xiao, J. Fan, and G. Zeng, Parameter estimation in quantum sensing based on deep reinforcement learning, *npj Quantum Inf.* **8**, 1 (2022).
- [13] D. W. Berry and H. M. Wiseman, Optimal States and Almost Optimal Adaptive Measurements for Quantum Interferometry, *Phys. Rev. Lett.* **85**, 5098 (2000).
- [14] D. W. Berry and H. M. Wiseman, Adaptive quantum measurements of a continuously varying phase, *Phys. Rev. A* **65**, 043803 (2002).
- [15] H. T. Dinani and D. W. Berry, Adaptive estimation of a time-varying phase with a power-law spectrum via continuous squeezed states, *Phys. Rev. A* **95**, 063821 (2017).
- [16] K. T. Laverick, H. M. Wiseman, H. T. Dinani, and D. W. Berry, Adaptive estimation of a time-varying phase with coherent states: Smoothing can give an unbounded improvement over filtering, *Phys. Rev. A* **97**, 042334 (2018).
- [17] Y. Aharonov, D. Z. Albert, and L. Vaidman, How the Result of a Measurement of a Component of the Spin of a Spin-1/2 Particle Can Turn Out to Be 100, *Phys. Rev. Lett.* **60**, 1351 (1988).
- [18] N. W. M. Ritchie, J. G. Story, and R. G. Hulet, Realization of a Measurement of a “Weak Value”, *Phys. Rev. Lett.* **66**, 1107 (1991).

- [19] J. Dressel, M. Malik, F. M. Miatto, A. N. Jordan, and R. W. Boyd, Colloquium: Understanding quantum weak values: Basics and applications, *Rev. Mod. Phys.* **86**, 307 (2014).
- [20] G. Chen, P. Yin, W. Zhang, G. Li, C. Li, and G. Guo, Beating standard quantum limit with weak measurement, *Entropy* **23**, 354 (2021).
- [21] L. Zhang, A. Datta, and I. A. Walmsley, Precision Metrology using Weak Measurements, *Phys. Rev. Lett.* **114**, 210801 (2015).
- [22] H. Li, G. Wang, B. Xia, Q. Song, J. Huang, and G. Zeng, High precision phase estimation with controllable sensitivity and dynamic range, *J. Phys. B: At., Mol. Opt. Phys.* **54**, 215503 (2021).
- [23] J. Huang, C. Fang, and G. Zeng, Weak-value-amplification metrology without spectral analysis, *Phys. Rev. A* **97**, 063853 (2018).
- [24] X. Qiu, L. Xie, X. Liu, L. Luo, Z. Li, Z. Zhang, and J. Du, Precision phase estimation based on weak-value amplification, *Appl. Phys. Lett.* **110**, 071105 (2017).
- [25] B. Xia, J. Huang, C. Fang, H. Li, and G. Zeng, High-Precision Multiparameter Weak Measurement with Hermite-Gaussian Pointer, *Phys. Rev. Appl.* **13**, 034023 (2020).
- [26] J. Martínez-Rincón, W. Liu, G. I. Viza, and J. C. Howell, Can Anomalous Amplification Be Attained Without Postselection?, *Phys. Rev. Lett.* **116**, 100803 (2016).
- [27] A. Monras, Optimal phase measurements with pure Gaussian states, *Phys. Rev. A* **73**, 033821 (2006).
- [28] J. Yu, Y. Qin, J. Qin, H. Wang, Z. Yan, X. Jia, and K. Peng, Quantum Enhanced Optical Phase Estimation with a Squeezed Thermal State, *Phys. Rev. Appl.* **13**, 024037 (2020).
- [29] A. A. Berni, T. Gehring, B. M. Nielsen, V. Händchen, M. G. Paris, and U. L. Andersen, Ab initio quantum-enhanced optical phase estimation using real-time feedback control, *Nat. Photonics* **9**, 577 (2015).